

Earthquake Risk Evaluation of Historic Masonry Buildings in Kathmandu Valley, Nepal

A. Furukawa, J. Kiyono & M. Tatsumi

Department of Urban Management, Kyoto University, Kyoto

K. Toki, H. Taniguchi & H. Parajuli

Disaster Mitigation of Urban Cultural Heritage, Ritsumeikan University, Kyoto



SUMMARY:

Kathmandu Valley is a center of culture in Nepal. Unfortunately, a large number of historic buildings have been damaged due to earthquakes in Kathmandu over the centuries since it is located on the earthquake-prone zone. Especially, an earthquake which hit Kathmandu in 1934 had a magnitude over 8 and it destroyed most of the cultural heritage, such as temples, shrines and monuments. Jatapol is an old area in Kathmandu where many historic masonry residential buildings are built without special attention to earthquake. It is very important to leave those buildings for posterity. To take measures to save those buildings from earthquakes, it is necessary to evaluate their seismic risk. However, there exist no sufficient statistical data to evaluate the risk from the past earthquakes. With this background, this study aims to numerically evaluate seismic risk of buildings using the refined version of the DEM.

Keywords: historic masonry building, earthquake risk, distinct element method

1. INTRODUCTION

Located on a part of the Himalayan orogen, Kathmandu Valley is a center of culture in Nepal. Unfortunately, a large number of historic buildings have been damaged due to earthquakes over the centuries since it is located on the earthquake-prone zone. Especially, an earthquake which hit Kathmandu in 1934 had a magnitude over 8 and it destroyed most of the cultural heritage, such as temples, shrines and monuments¹⁾.

Kathmandu Valley was designated as World Heritage Site by UNESCO in 1979. However, as the industrialization and commercialization proceeds, more historic masonries with tiled roofs and composite buildings of masonry and timber were demolished, and more concrete buildings with low quality constructed. Therefore, Kathmandu Valley was registered in a list of Cultural Heritage in Danger in 2003. Owing to the brave effort by World Heritage Committee and associated ministries of Nepal afterwards, it was unlisted in 2007²⁾.

In this way, many efforts have been made from the view point of the protection of the cultural heritage²⁾, however, an effort of protecting them from earthquake disasters has not been made sufficiently. Damaged historic monuments, temples and shrines have been demolished or reconstructed into reinforced concrete buildings with no historic value.

Japanese government has been providing technical assistance through JICA. In 2002, seismic damage to buildings in Kathmandu is estimated by a simple method utilizing a structural vulnerability function³⁾. However, since the used vulnerability function is statistically constructed from the past earthquake data worldwide, it is not necessarily suitable for Kathmandu. Moreover, since the vulnerability function is mainly constructed by damaged residential buildings, it is not necessarily suitable for historic buildings, either. Therefore, seismic resistance of existing historic buildings in Nepal is still unclear.

With this background, this study conducts seismic simulation of existing historic masonry buildings in Jhatapo area, Kathmandu by the use of the refined version of the DEM. Their seismic risk is evaluated by the damage index proposed by Okada and Takai⁴⁾.

2. ANALYSIS METHOD

2.1 Refined version of DEM⁵⁾

This study employs a refined version of DEM to simulate a series of structural dynamic behaviors from elastic to failure to collapse phenomena. A structure is modeled as an assembly of rigid elements, and interaction between elements is modeled with multiple springs and multiple dashpots that are attached to the surfaces of elements. Fig. 1 (a) shows a spring for computing the restoring force (restoring spring), which models the elasticity of elements. The restoring spring is set between continuous elements. Fig. 1 (b) shows a spring and dashpot for computing the contact force (contact spring and dashpot) and modeling the contact, separation and recontact between elements. The dashpots are introduced to express energy dissipation due to the contact. Structural failure is modeled as breakage of the restoring spring (Fig. 1 (c)), at which time the restoring spring is replaced with a contact spring and a contact dashpot (Fig. 1 (b)). Structural collapse behavior is obtained using these springs and dashpots. The elements shown in Figs. 1 (a) and (b) are rectangular parallelepipeds, but the method does not limit the geometry of the elements. The surface of an element is divided into small segments as shown in Fig. 1 (d). A segment in the figure is rectangular, but the method does not limit the geometry of the segment. The black points indicate the representative point of each segment, and the relative displacement or contact displacement between elements is computed for these points. Such points are referred to as contact points or master points in this study. One restoring spring and one combination of contact spring and dashpot are attached to one segment (Fig. 1 (e)) at each of the representative points in Fig. 1 (d). The spring constant for each segment is derived on the basis of the stress–strain relationship of the material and the segment area. Forces acting on each element are obtained by summing the restoring force, contact force and other external forces such as the gravitational force and inertial force of an earthquake. The behavior of an element consists of the translational behavior of the center of gravity and the rotational behavior around the center of gravity. The translational and rotational behaviors of each element are computed explicitly by solving Newton's law of motion and Euler's equation of motion.

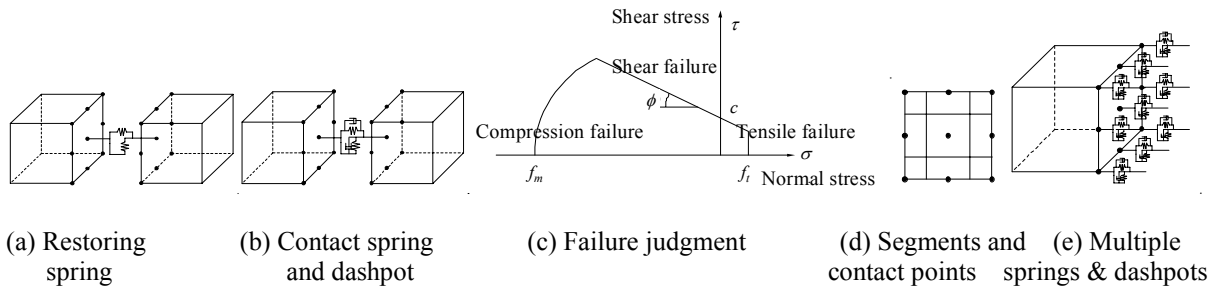


Figure 1 Basic concept of analysis method

2.2 Spring constant of each element

There are two types of springs, namely restoring and contact springs. It is considered that each segment has its own spring. The springs are set for both the normal and shear directions of the surface. The spring constants per area in the normal and shear directions, k_n and k_s , are obtained as follows.

$$k_n = \frac{E}{(1-\nu^2)\ell} \quad k_s = \frac{E}{2(1+\nu)\ell} \quad (2.1)$$

where E is Young's modulus, ν is Poisson's ratio, and ℓ is the distance from the surface at which the spring is connected to the center of gravity.

2.3 Modeling of elastic behavior

It is assumed that two elements, A and B , are continuous, and that a contact point of element A is continuous with element B . Let G_A and G_B be the centers of gravity of elements A and B respectively. Let ℓ_A be the distance from G_A to the surface of element A in contact. Let ℓ_B be the distance from G_B

to the surface of element B in contact. Let E_A and E_B be Young's moduli and ν_A and ν_B be Poisson's ratios of elements A and B .

The spring constants per area for the elements A and B are obtained from Eq.(2.1). Assuming that these springs are connected in series, the spring constants between elements per area, \bar{k}_n and \bar{k}_s , are

$$\bar{k}_n = \frac{1}{\frac{\ell_A}{E_A/(1-\nu_A^2)} + \frac{\ell_B}{E_B/(1-\nu_B^2)}}, \quad \bar{k}_s = \frac{1}{\frac{\ell_A}{E_A/2(1+\nu_A)} + \frac{\ell_B}{E_B/2(1+\nu_B)}} \quad (2.2)$$

The spring constant between elements connected by mortar is also obtained in a similar manner. For example, in masonry structures, bricks are often connected with mortar. In such cases, the spring constant per area between elements (bricks) is obtained as

$$\bar{k}_n = \frac{1}{\frac{\ell_A - t_M/2}{E_A/(1-\nu_A^2)} + \frac{t_M}{E_M/(1-\nu_M^2)} + \frac{\ell_B - t_M/2}{E_B/(1-\nu_B^2)}}, \quad \bar{k}_s = \frac{1}{\frac{\ell_A - t_M/2}{E_A/2(1+\nu_A)} + \frac{t_M}{E_M/2(1+\nu_M)} + \frac{\ell_B - t_M/2}{E_B/2(1+\nu_B)}} \quad (2.3)$$

where t_M is the mortar thickness and E_M is Young's modulus and ν_M is Poisson's ratio of the mortar. The normal direction of forces is the direction perpendicular to the surface of the master point of element A .

Let σ and τ be the normal and shear stresses acting at the contact point, and u_n and u_s be the relative displacements between the adjacent master and slave points in the normal and shear directions. The relation between traction (σ, τ) and relative displacements (u_n, u_s) is then written as

$$\sigma = \bar{k}_n u_n, \quad \tau = \bar{k}_s u_s. \quad (2.4)$$

The method cannot handle the poisson's effect since it considers the contact between two elements.

2.4 Modeling of failure phenomena

The elastic behavior of structures is demonstrated by the multiple restoring springs between continuous elements until the restoring force of a spring reaches its elastic limit. The elastic limits are modeled using criteria of tension, shear and compression failure. When a spring reaches one of these limits, it is judged that failure has occurred at the segment of the spring. After the failure, the restoring spring is replaced with a contact spring and dashpot at this segment. The method can trace the expansion of failure between elements. The three failure modes—namely, tension, shear and compression failure modes—are defined as follows.

2.4.1 Tension failure mode

In the tension failure mode, the parameter considered is the tensile strength f_t . When the normal stress of a spring σ exceeds the tensile strength, the restoring spring is assumed to be broken by the tension failure. The yield function has the following form (Fig. 1(c)).

$$f_1(\sigma) = \sigma - f_t \quad (2.5)$$

The normal restoring stress cannot exceed this limit.

2.4.2 Shear failure mode

For the shear failure mode, the Coulomb friction envelope is used. The parameters considered are the bond strength c and friction angle ϕ . The yield function has the following form (Fig. 1(c)).

$$f_2(\sigma) = |\tau| + \sigma \tan \phi - c \quad (2.6)$$

The shear restoring stress cannot exceed this limit.

2.4.3 Compression failure mode

For the compression mode, an ellipsoid cap model is used. The yield function has the form (Fig. 1(c)) as.

$$f_3(\sigma) = \sigma^2 + C_s \tau^2 - f_m^2 \quad (2.7)$$

where f_m is the compressive strength and C_s is the material model parameter. $C_s = 9$ is adopted on the basis of past research⁶⁾. When the restoring stress exceeds this limit, both the normal and shear restoring stresses are reduced in the same proportion to meet this limit.

2.5 Modeling of contact and recontact between elements

If a segment of an element is in contact with another element with which the segment is not continuous via the restoring spring, the contact spring and dashpot generate the contact force. Contact

between a segment and the surface of another element is detected at each time step for all segments that are not continuous with other elements via a restoring spring. The spring constant and the contact forces in the normal and shear directions are calculated in the same manner as for the restoring force. The differences from the case for the restoring force are that the contact force is generated only while the compression force acts and that the shear force is bounded by the friction limit.

$$\tau = \sigma \tan \phi \quad (2.8)$$

where ϕ is the friction angle. The dashpot is introduced to express the energy dissipation of the contact. The damping coefficient per area is calculated as follows.

$$c_n = 2h_n \sqrt{m_{ave} k_n}, \quad c_s = 2h_s \sqrt{m_{ave} k_s} \quad (2.9)$$

where h_n and h_s are the damping constants for the normal and shear directions. m_{ave} is the equivalent mass per area relevant to this contact. In this study, m_{ave} is calculated as

$$m_{ave} = \rho_A l_A + \rho_B l_B \quad (2.10)$$

where ρ_A and ρ_B are the mass densities of elements A and B . The damping constants should be evaluated according to the properties of the elements, but this study adopts critical damping ($h_n = h_s = 1.0$) by considering that most structural components tend not to bounce greatly and their oscillation tends to disappear quickly when they collide with each other.

2.6 Equations of Motion

The equations of motion can be constructed using the restoring and contact forces and other external forces. The motion of each element is obtained by solving the two equations of motion. One is the equation for the translational motion of the center of gravity, and the other is the equation for the rotational motion around the center of gravity. By solving the equations of motion step by step, the position of each element can be traced, and the whole structural behavior can be obtained.

3. ANALYSIS OUTLINE

3.1 Jhatapo area

Our target area is Jhatapo area shown in Fig. 2. The buildings are classified by number of stories and building types. There are many historic masonry buildings in the target area as shown in Fig.3, and most of them are unreinforced masonry buildings which have the high possibility to get severe damage during earthquakes. There are some confined masonry buildings with reinforced concrete.

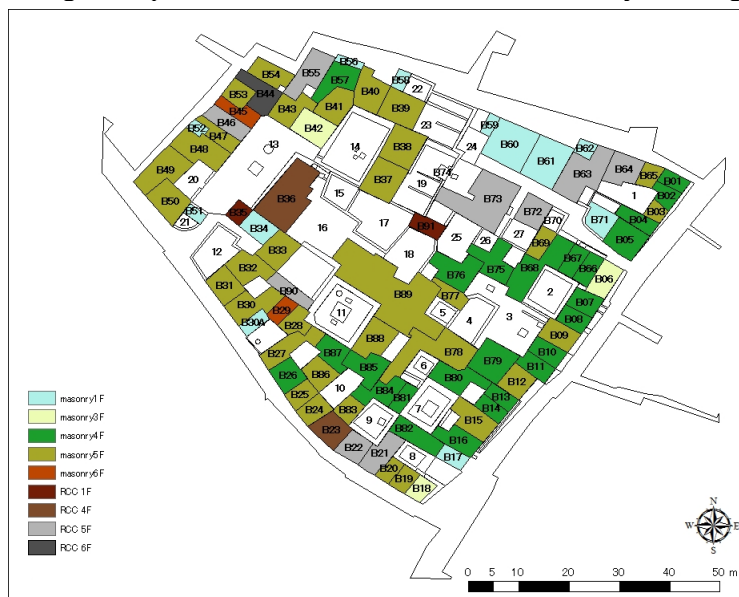
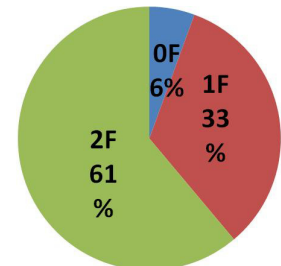
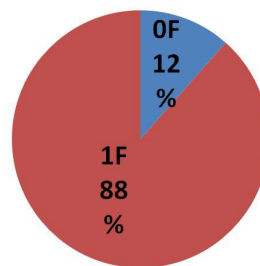
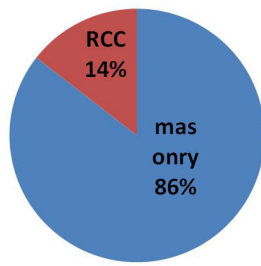
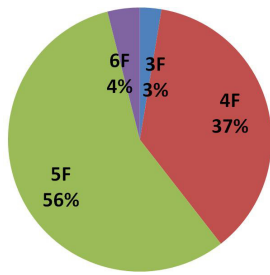


Fig.2 Target area (Jhatapo area)



Fig.3 Typical buildings in the target area



(a) by number of stories (b) by building type
Fig.4 Classification by number of stories and building type

(a)4-story masonry buildings (b)5-story masonry buildings
Fig. 5 Number of additional stories

3.2 Complete enumeration

A complete enumeration was done for the buildings in the target area. There are 13 one-story buildings, but they are neglected since they are vacant buildings or no-residential buildings.

When the buildings are classified with the number of stories, the ratio of the 3, 4, 5 and 6-story buildings are 3, 37, 56 and 4%, respectively as shown in Fig. 4(a). The 4 or 5-story buildings occupy 93% of the buildings. The number of buildings with 3 and 6 stories is scant, and there are no buildings with two stories.

When the buildings are classified with the building type, 86% of the buildings are unreinforced masonry, and the other buildings are confined masonry with reinforced concrete as shown in Fig.4(b).

Most of the buildings experienced an addition of stories to the original buildings. All of the 5 or 6-story buildings experienced the addition of stories. The number of added stories for 4 and 5-story buildings are shown in Fig. 5. From the figure, most buildings were originally 3 story buildings before the addition.

Finally, the buildings are classified into 7 types by the number of stories and building types as shown in Fig. 6. They are the masonry buildings with 3, 4, 5 and 6 stories, and the confined masonry buildings with reinforced concrete (RCC) of 4, 5 and 6 stories. We made 7 analytical models according to this classification, and estimated the seismic risk.

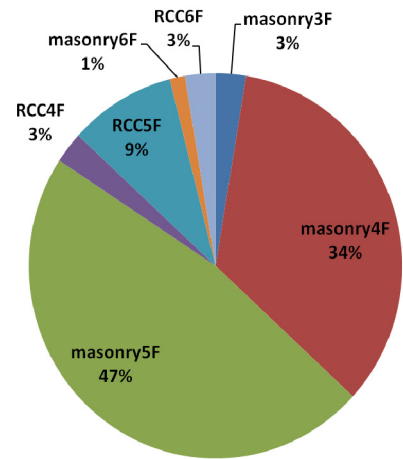
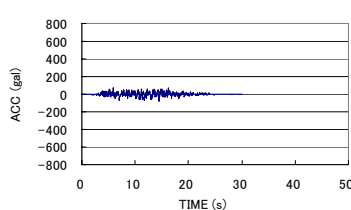


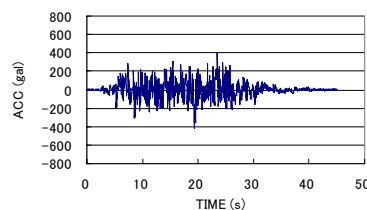
Fig.6 Classification of buildings

3.3 Input ground acceleration

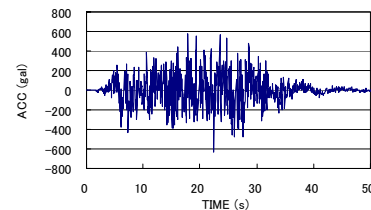
Input ground acceleration is shown in Fig. 7. These are estimated from the Nepalese historic seismic data and active fault data by seismic hazard analysis⁷. Fig. 7(a) is an acceleration with the occurrence probability of 40% in 50 years (return period is 98 year) and has the peak acceleration of 84 gal. Fig. 7(b) is an acceleration with the occurrence probability of 10% in 50 years (return period is 475 year) and has the peak acceleration of 420 gal. Fig.7(c) is an acceleration with the occurrence probability of 5% in 50 years (return period is 975 year) and has the peak acceleration of 630 gal.



(a) 40% (98year)



(b) 10%(475 year)



(c) 5% (975year)

Fig. 7 Input ground acceleration with respective occurrence probability in 50 years (Return period)

3.4 Seismic risk evaluation

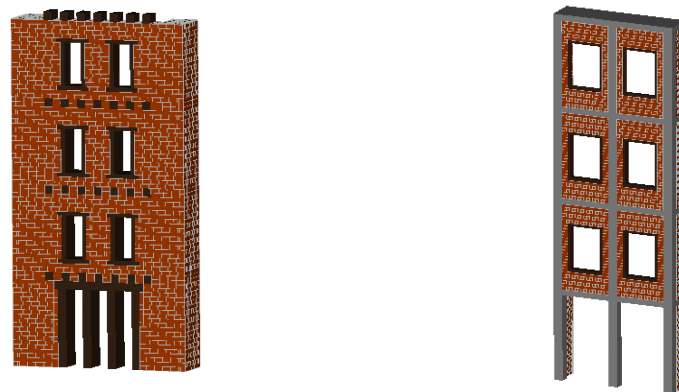
3.4.1 Analytical modeling

All buildings are continuous and shear the party walls with the adjacent buildings as shown in Fig.3. According to the previous study by D'Ayala⁸⁾, they assume damage to façade for this type of continuous buildings. Therefore, we considered that the failure to the façade is the dominant failure mode and numerically estimated the damage to façade. The ground motion is input in the out-of-plane direction of the buildings.

We made 7 analytical models according to the classification. The analytical models for a 4-story masonry building and a 4-story confined masonry building with reinforced concrete are shown in Fig.8. The size of each brick is 10cm x 10cm x 20cm. The façade and side wall of 1m are modeled. The back of the side wall is supposed by the fixed elements which cannot be seen in Fig. 8.

For masonry buildings, each story is 2.0m high, and the width is 4.2m. The floor of each floor is composed of timber beams, The stories higher than 3rd floor is considered to be added, and the depth of the wall is 60cm for 1st-3rd floors, and 40cm for floors higher than 4th floor based on the interviews to the local people. For confined masonry buildings, each story is 3.0m high, the width is 4.1m, and the section of RC frame is 30cm x 30cm. The depth of the wall is 20cm for 1st-3rd floors, and 10cm for floors higher than 4th floor.

The parameters used are shown in Table 1. The time interval is 4.0×10^{-5} sec for masonry buildings, and 1.0×10^{-5} sec for confined masonry.



(a) 4-story masonry building

(b) 4-story confined masonry building

Fig. 8 Analytical models

Table 1 Material properties and failure criteria

Variable	Adobe Brick	Mortar	Wood	RC
Mass density (kg/m^3)	1.8×10^3	-	7.0×10^2	2.3×10^3
Young's modulus (N/m^2)	2.7×10^8	2.7×10^8	6.3×10^8	2.5×10^{10}
Poisson's ratio	0.11	0.25	0.3	0.2
Tensile strength f_t (N/m^2)	-	0.0	1.1×10^8	1.91×10^6
Shear strength c (N/m^2)	-	9.0×10^4	9.0×10^6	2.2×10^6
Friction angle ϕ	-	42.5°	0°	32°
Compressive strength (N/m^2)	-	1.58×10^6	4.5×10^7	2.4×10^7

3.4.2 Damage index

To evaluate structural damage, damage index proposed by Okada and Takai as shown in Fig.9 and Table 2 is used⁴⁾. Coburn summarized the progression of damage to the masonry structural system and damage grade as shown in Fig. 9⁹⁾, and then Okada and Takai scored damage index which takes between 0 (No damage) and 1 (Total Collapse) for each damage grade according to the definition by the European Macroseismic Scale 1998 (EMS98)¹⁰⁾.

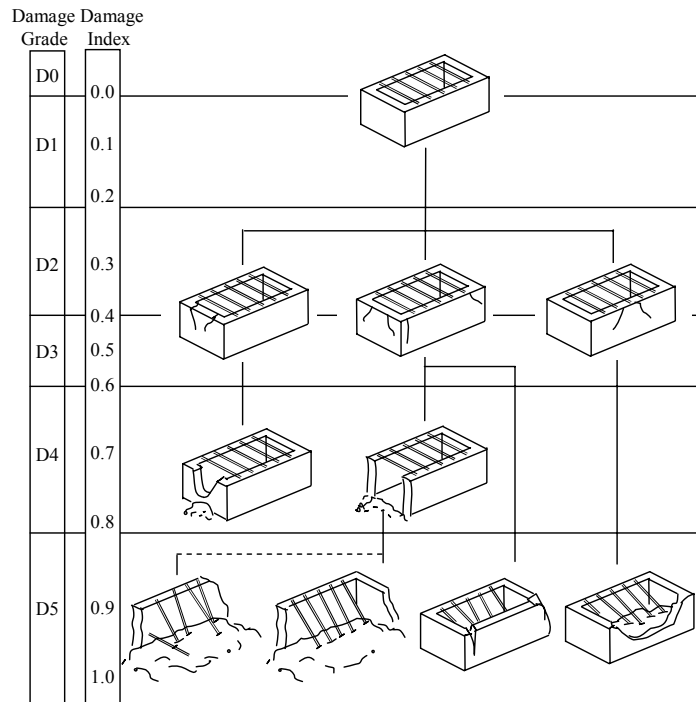


Fig.9 Damage pattern and its relevant damage index^{4),9)}

Table 2 Damage index and classification of damage to masonry buildings (EMS98)¹⁰⁾

Damage Grade	Damage Index	Damage Description	Damage State
D0	0.0	No damage	No damage
D1	0.0~0.2	Negligible to sight damage	Hair-line cracks in very few walls. Fall of small pieces of plaster only. Fall of loose stones from upper parts of buildings in very few cases.
D2	0.2 ~ 0.4	Moderate damage	Cracks in many walls. Fall of fairly large pieces of plaster. Partial collapse of chimneys.
D3	0.4 ~ 0.6	Substantial to heavy damage	Large and extensive cracks in most walls. Roof tiles detach. Chimneys fracture at the roof line; failure of individual non-structural elements (partitions, gable walls).
D4	0.6 ~ 0.8	Very heavy damage	Serious failure of walls, partial structural failure of roofs and floors
D5	0.8 ~ 1.0	Destruction	Total or near total collapse

4. Results

4.1 Seismic behavior

Three input ground motions with different occurrence probability is input to 7 models. Some of the results are shown in Figs. 10-13. Since the ground motion is input in the out-of-plane direction of the façade, the façade of the masonry buildings vibrated in the out-of-plane direction and failed. This made the side walls fall down and there are many fallen bricks around the buildings. From Figs. 10-12, it is found that the masonry buildings can avoid collapse for the earthquakes with the occurrence probability of 40% in 50 years, but they experience sever damage against the earthquakes with the occurrence probabilities of 10 and 5% in 50 years. It is also found that the higher building has suffered from more severe damage. Confined masonry buildings with the reinforced concrete could avoid collapse for three ground motions.

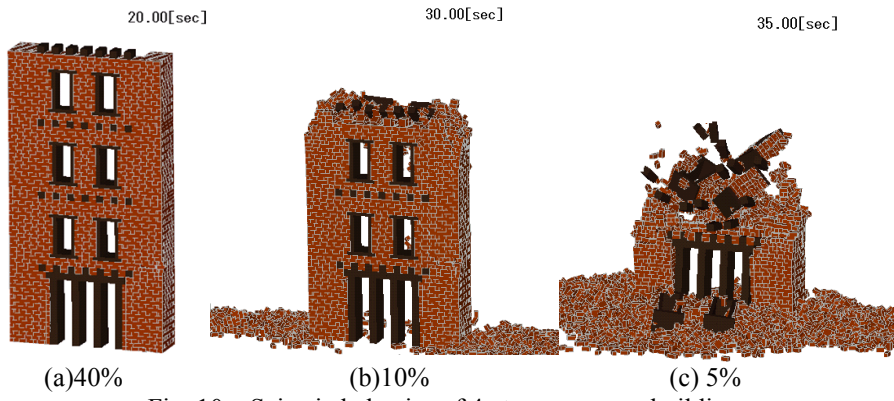


Fig. 10 Seismic behavior of 4-story masonry buildings

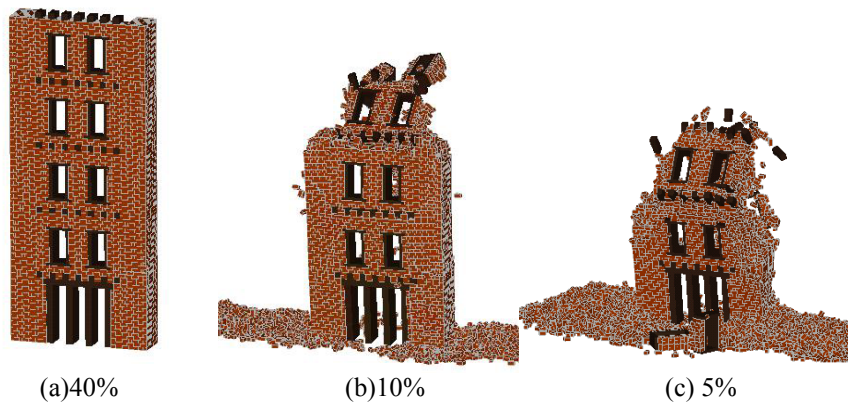


Fig. 11 Seismic behavior of 5-story masonry buildings

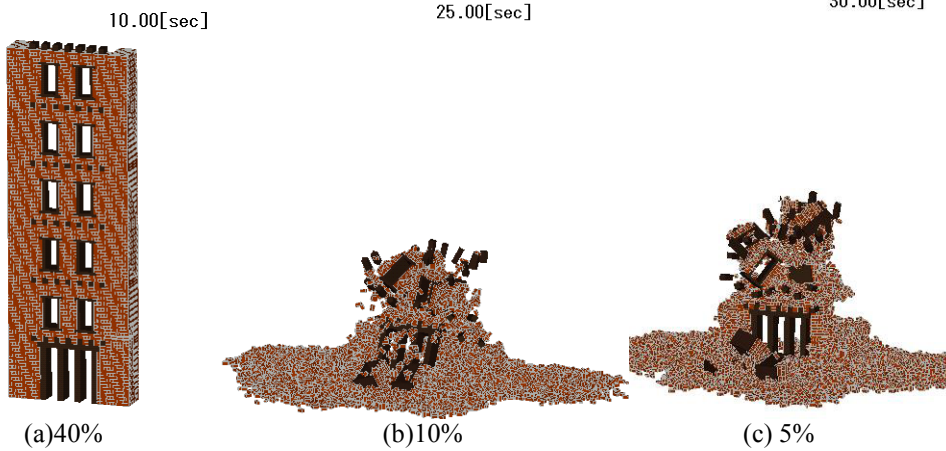


Fig. 12 Seismic behavior of 6-story masonry buildings

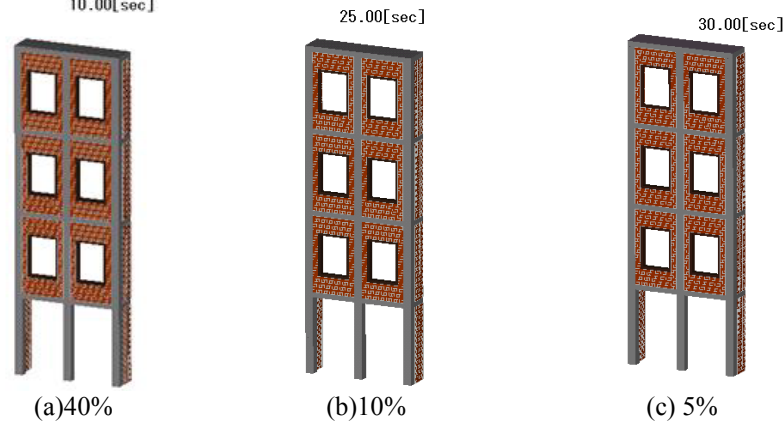
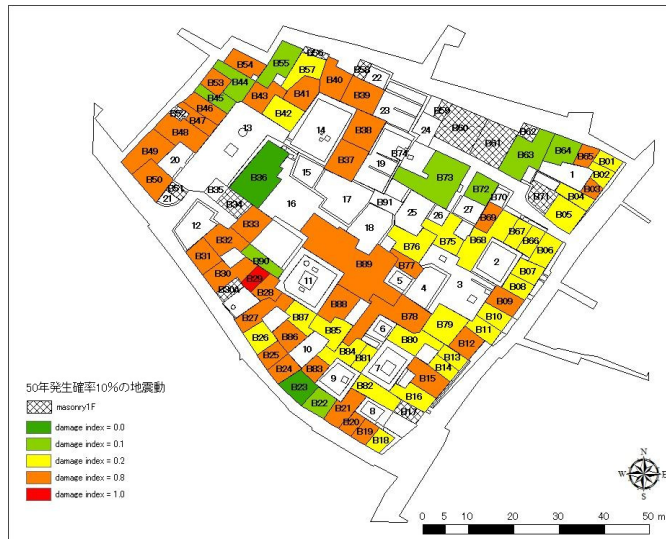


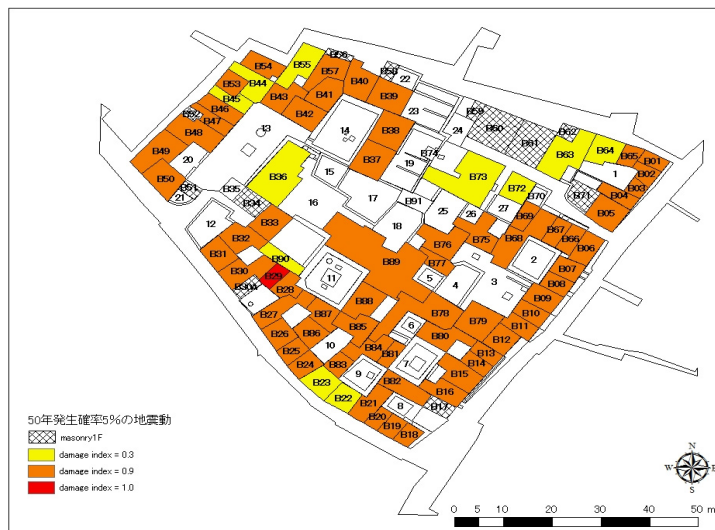
Fig. 13 Seismic behavior of 5-story confined masonry buildings



(a) Occurrence probability of 40% in 50 years



(b) Occurrence probability of 10% in 50 years



(c) Occurrence probability of 5% in 50 years

Fig. 14 Estimated damage index for target area

4.2 Mapping

By comparing the structural damage as shown in Figs.10-13 with Fig.9, the damage indices of 7 classified buildings are visually judged for three input ground motions. The results are mapped as shown in Fig.14. The shaded buildings in Fig.14 are one-story buildings. For the input ground motion with the occurrence probability of 40% in 50 years, most of the buildings survive without collapse. However, for the ground motion with the occurrence probabilities of 10 and 5%, most masonry buildings suffer very heavy damage or destruction and the confined masonry buildings experience moderate damage.

5. CONCLUSION

The seismic risk of buildings in the Jhatapo area is evaluated by using the refined version of DEM. The complete enumeration was done and the buildings are classified into 7 types with different building types and the number of stories. Only the façade is modeled for the analysis assuming that the vibration in the out-of-plane direction is dominant. The input ground motion with three different occurrence probabilities are input in the out-of-plane direction of the models, and the structural damage is evaluated by using the damage index. It is found for the ground motion with the occurrence probabilities of 10 and 5%, most masonry buildings suffer very heavy damage or destruction and the confined masonry buildings experience moderate damage. As the number of stories increases, the structural damage becomes severer.

ACKNOWLEDGEMENTS

This work was supported by a Grant-in-Aid for the Global COE Program “Global COE for Education, Research and Development of Strategy for Disaster Mitigation of Cultural Heritage and Historic Cities (Ritsumeikan University)” from the Ministry of Education, Culture, Sports, Science and Technology of Japan.

REFERENCES

- 1) Amatya, S.: Monument conservation in Nepal, Vajra Publications, 2008.
- 2) Rohit K.R.: Heritage homeowner’s preservation handbook, UNESCO, 2007.
- 3) JICA: Final Report of JICA Study Team on Kathmandu Valley Earthquake Disaster Mitigation Planning, 2002.
- 4) Okada S, Takai N.: The basic framework for casualty modeling of victims of earthquake, (1) Classification of structural types and damage patterns of buildings, and damage index function, *Reports of the Tono Research Institute of Earthquake Science*, No. 2, pp.12-23 (in Japanese with English abstract), 1999.
- 5) Furukawa, A., Kiyono, J., Toki, K.: Proposal of a numerical simulation method for elastic, failure and collapse behaviors of structures and its application to masonry walls, *Journal of Disaster Research*, Vol.6, No.1, Paper: Dr6-1-4524, 2011.
- 6) Lourenco, P.B.: Analysis of masonry structures with interface elements, theory and applications, Delft University of Technology, Faculty of Civil Engineering, TU-DELFT report no.03-21-22-0-01, TNO-BOUW report no.94-NW-R0762, 1994.
- 7) Parajuli, H.R., Kiyono, J., Ono, Y., and Tsutsumiuchi, T.: Design earthquake ground motions from probabilistic response spectra: Case study of Nepal, *Journal of Japan Association for Earthquake Engineering*, Vol.8, No.4, pp.16-28, 2007.
- 8) D’Ayala, D.: Correlation of fragility curves for vernacular building types: Houses in Lalitpur, Nepal and in Istanbul, Turkey. In: Proceedings of the 13th World Conference of Earthquake Engineering, Vancouver Canada, 2004.
- 9) Coburn, A.W.: Seismic vulnerability and risk reduction strategies for housing in eastern Turkey. Ph. D. Thesis, The Martin Centre for Architectural and Urban Studies, University of Cambridge, United Kingdom, 1987.
- 10) Grünthal, G. (ed.): European Macroseismic Scale 1998 (EMS-98), http://www.gfz-potsdam.de/portal/gfz/Struktur/Departments/Department+2/sec26/resources/documents/PDF/EMS-98_Original_englisch_pdf, 1998.